Band-Gap Opening in Metallic Single-Walled Carbon Nanotubes by Encapsulation of an Organic Salt

B. Nieto-Ortega, J. Villalva, M. Vera-Hidalgo, L. Ruiz-González, E. Burzurí, E. M. Pérez

Band gap opening in metallic single-walled carbon nanotubes by encapsulation of an organic salt

Belén Nieto-Ortega,[a] Julia Villalva,[a] Mariano Vera-Hidalgo,[a] Luisa Ruiz-González,[b] Enrique Burzurí*[a] and Emilio M. Pérez*[a]

Abstract We show that the encapsulation of viologen derivatives into metallic SWNTs results in the opening of a band gap, making the SWNTs semiconducting. Raman spectroscopy, thermogravimetric analysis and aberration corrected high resolution transmission electron microscopy confirm the encapsulation process, and through the fabrication of field-effect transistor devices, we prove the change of the electronic structure of the tubes from metallic to semiconductor upon the encapsulation. The opening of a gap in the band structure of the tubes was not detected in supramolecular controls.

Carbon nanotubes (CNTs) are one of the most promising one-dimensional nanoscale materials with potential applications in the fields of nanoelectronics,[1] optoelectronics[2] and medical (bio)technologies.[3] Interestingly, their optical,[4] electronic[5] and mechanical[6] properties can be modulated on demand *via* controlled chemical modification.[7] Thanks to the versatility of synthetic chemistry, a broad variety of strategies have been employed to functionalize carbon nanotubes. Making strong covalent bonds to the walls of CNTs[7a, 8] provides remarkable stability but at the expense of substantial distortion of the nanotubes' 1D structure. On the other hand, non-covalent derivatives[9] traditionally mediated *via* van de Waals interactions with the outer surface of the SWNTs, preserve the 1D structure but are typically labile under external manipulation.

An interesting alternative is the noncovalent modification to form rotaxane-like structures, in which macrocycles are clipped around the SWNTs to yield mechanically interlocked derivatives of SWNTs (MINTs).[10] MINTs show extreme thermal stability because the macrocycles cannot be separated from the SWNTs without breaking a covalent bond. A final possibility is to introduce molecules inside the cavities of the SWNTs *via* endohedral encapsulation, which also results in particularly stable noncovalent derivatives.[11] In fact, the three distinctive characteristics of the mechanical bond, namely stability, topology and dynamic properties are present in endohedral derivatives of carbon nanotubes (X@SWNTs).[12] As an additional advantage, the endohedral modification of SWNTs also keeps the external SWNT surface free for interaction with the surroundings or even for further chemical modification.

[a] Dr. B. Nieto-Ortega, J. Villalva, M. Vera-Hidalgo, Dr. E. Burzurí, Prof. E. M. Pérez
IMDEA Nanoscience,
Ciudad Universitaria de Cantoblanco, c/Faraday 9, 28049 Madrid, Spain
E-mail: emilio.perez@imdea.org; enrique.burzuri@imdea.org;

[b] Prof. L. Ruiz-González
Departamento de Química Inorgánica,
Universidad Complutense de Madrid, Madrid, Spain

Supporting information for this article is given via a link at the end of the document.

Here, we report that the encapsulation of viologen derivatives into metallic SWNTs results in the opening of a band gap, making the SWNTs semiconducting. We show that the endohedral modification is robust enough to survive thorough washing of the sample. By using *ac*-dielectrophoresis, we prepared Field-Effect Transistor (FET) devices and performed electron transport measurements through the endohedral derivatives. We show that the electronic band structure of the initially metallic SWNTs is switched from metallic to a high-quality, homogeneous and robust semiconductor, in contrast with adequate supramolecular controls. The resulting FET-like device displays back-to-back Schottky diode behavior.

Viologens, which are derived of 1,1'-disubtitued-4,4'-bipyridinium, were chosen for their well-known electron transport properties,[13] and because they have previously been used as doping agents of carbon-based materials in a supramolecular configuration.[14] In particular, we synthesized didodecyl-4,4'-bipyridinium dihexafluorophosphate (**Viol** in Figure 1a, see SI for synthetic details). Its low solubility in common organic solvents facilitates encapsulation inside the SWNTs thanks to solvophobic effects. Metallic SWNTs with diameter from 1.6 to 2.2 nm (length 3−30 μm, 99% purity) were used for the salt encapsulation in this study.[15] A schematic illustration of **Viol** encapsulation in a 1.8 nm-wide metallic carbon nanotube is shown in Figure 1b.

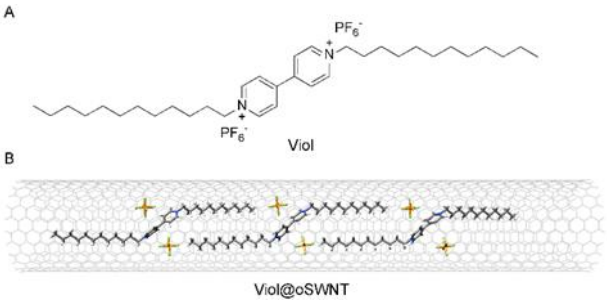

Figure 1. (a) Chemical structure of 1,1'-didodecyl-4,4'-bipyridinium dihexafluorophosphate (**Viol**). (b) Model illustration of **Viol** inside a metallic SWNT of 1.8 nm diameter. The PF_6 anions are drawn inside the nanotube, but since they are not clearly visible in the AC-HRSTEM images (see below) they could potentially be outside.

Commercial SWNTs are end-closed and therefore need to be opened as a previous step to encapsulate the organic salt. In short, the SWNTs were opened by heating them in air at 400 °C for 3 h up to a total weight loss of 20%. Spurious catalytic nanoparticles were also removed in the process. The powder obtained was annealed at 800 °C for 1 hour in vacuum to remove any functional groups, which can block the SWNT opened ends. Opened SWNTs are hereafter labelled as oSWNTs as opposed to pristine, end-closed SWNTs.

Encapsulation of the **Viol** into the oSWNTs was performed following the procedure described by Yanagi *et al* for similar molecules.[15c, 15d] Briefly, pure **Viol** sample (70 mg) was dissolved in N,N-dimethylformamide (DMF) and the oSWNTs (7 mg) were added to the solution. The mixture was refluxed overnight under N_2 atmosphere. Thereafter the solution was filtered and washed with DMF several times to remove any non-encapsulated **Viol**. We call the complexes produced in this way **Viol**@oSWNT ('@' refers to filling). A reference sample was prepared following the same procedure but using raw, end-closed SWNTs in which the **Viol** cannot be encapsulated. We call this reference complex **Viol**-SWNT.

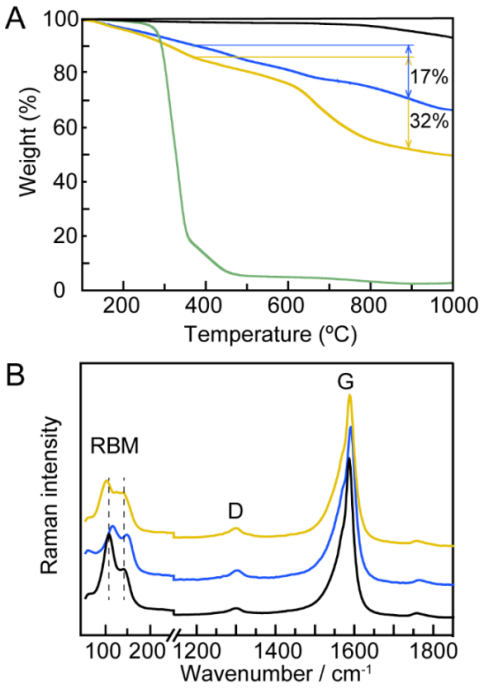

Figure 2. (a) TGA analysis (N_2, 10 ºC min^{-1}) of oSWNT (black), **Viol**-SWNT (blue), **Viol**@oSWNT (golden) and **Viol** (green). (b) Raman spectra (λ_{exc}=785 nm) of oSWNT (black line), **Viol**-SWNT (blue) and **Viol**@oSWNT (golden).

A first indication of the encapsulation is obtained from thermogravimetric analysis (TGA). Figure 2a presents the weight loss curve of **Viol**@oSWNT sample in comparison with the pure **Viol** powder, **Viol**-SWNT and oSWNTs. The oSWNT sample does not decompose under N_2 atmosphere while the pure **Viol** sample decomposes completely at ~470 ºC. In the **Viol**@oSWNT sample, we observe a new decomposition component not present in oSWNT, that appears at high temperatures (790 ºC). We tentatively ascribe this step to the de-encapsulation/decomposition of the **Viol**, as indicated by the shift to significantly larger temperatures when compared to bare **Viol**, suggesting that the organic salt is protected by the tube. This analysis is supported by the absence of this step in the **Viol**-SWNT supramolecular hybrids. Note that both the **Viol**@oSWNT and the **Viol**-SWNTs samples show a not very well defined weight-loss that extends from 200 to 500 ºC, which we attribute to residual DMF and/or adsorbed **Viol**. The total **Viol** mass loss in the **Viol**@oSWNT sample is around 32%, ~15% with respect to **Viol**-SWNT reference sample. This corresponds to the presence of 1 organic salt molecule every 250-300 carbon atoms of oSWNT.

The Raman spectra of oSWNT, **Viol**-SWNT and **Viol**@oSWNT (λ_{exc} = 785 nm) are compared in Figure 2b. Further Raman characterization is shown in the Supporting Information. All spectra are very similar with no increase in the relative intensity of the D band, which confirms that the covalent structure of the oSWNT is preserved upon functionalization. We do not observe any significant changes in the wavenumber of the G band upon the formation of **Viol**@oSWNT, either, which suggests that doping of the SWNTs by the encapsulated **Viol** is not significant in the ground state. The radial breathing modes (RBMs), on the other hand, show very interesting changes. The reference oSWNT sample shows two main RBMs, centered at 112 cm^{-1} and 144 cm^{-1}, respectively. The same peaks are observed in the spectrum of **Viol**-SWNT, although both are blue-shifted by 8 cm^{-1}. Both peaks are shifted in the same direction and to the same extent, suggesting that these changes may be due to a different degree of aggregation in the sample after the chemical treatment. In contrast, the RBM region of **Viol**@oSWNT, shows three peaks, at 107 cm^{-1}, 129 cm^{-1} and 143 cm^{-1} respectively. The appearance of a new RBM, together with the redshift of the peak corresponding to the larger diameter SWNTs, while the peak corresponding to the thinner SWNTs stays in place, suggests that there is a significant change upon encapsulation of **Viol** and that it affects the larger nanotubes to a greater extent.

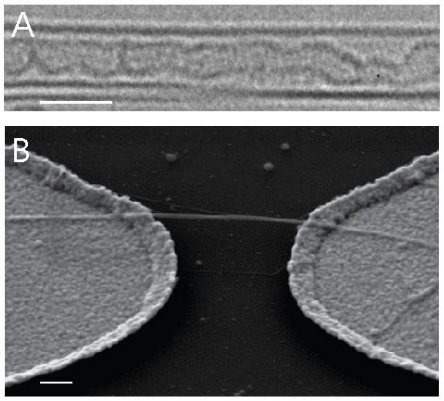

Figure 3. (a) Representative AC-HRSTEM image of **Viol**@oSWNT. Scale bar is 2 nm. (b) Scanning Electron Microscopy (SEM) image of a **Viol**@oSWNT bridging two metallic Au electrodes. Scale bar is 200 nm.

Direct evidence for the encapsulation of **Viol** molecules in the oSWNTs was provided by aberration corrected high-resolution transmission electron microscopy (AC-HRTEM) (see SI).[16] An AC-HRTEM image of **Viol**@oSWNT is shown in Figure 3a. Low energy (60 keV) and dose set were used to minimize the commonly knock-on damage in molecular structures due to the electron beam (e-beam).[17] Imaging at high magnification reveals that the nanotube cavities are filled with molecular material. Despite the good quality of the images, we are not able to elucidate the exact disposition of our molecules inside the carbon nanotube, due to e-beam induced Brownian motion of the **Viol** guests or even to their fast decomposition under the e-beam.[18]

The electronic properties of **Viol**@oSWNT have been measured in tens of field-effect transistor (FET)-like devices.

Series of 400-nm spaced source-drain electrodes are fabricated by optical lithography and subsequent Au evaporation on Si substrates coated with 300 nm of SiO_2. Tens of these electrodes are connected to a common Au pad so that tens of **Viol**@oSWNT FETs can be electrically probed simultaneously (see scheme of the multielectrode device in the Supporting Information). **Viol**@oSWNT, **Viol**-SWNT and oSWNT are trapped and aligned between the electrodes by *ac*-field dielectrophoresis.[19] In short, an *ac*-electric field is applied between the electrodes immersed in a tetrachloroethane solution containing a dispersion of the nanotubes sample. Voltage, *ac*-frequency and time parameters are optimized to maximize the yield of a single tube per electrode pair (see Supporting Information). Figure 3b shows a representative Scanning Electron Microscopy (SEM) image of one of the devices. The two electrodes are bridged by **Viol**@oSWNT that is visible thanks to the enhanced apparent diameter provided by voltage contrast with the substrate.[20]

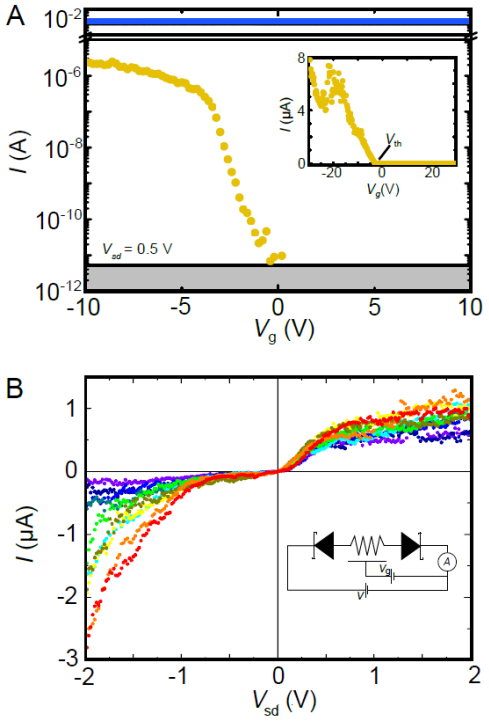

Figure 4. (a) Transfer characteristics of **Viol**@oSWNT (golden), **Viol**-SWNT (blue) and bare oSWNT (black) FET devices measured at V_{sd} = 0.5 V. Clear p-doped semiconducting behavior with 10^6 on-off ratio can be observed for **Viol**@oSWNT. In contrast, **Viol**-SWNT and oSWNT FETs show no gate dependence as expected in metals. The estimated carrier mobility in **Viol**@oSWNT is $\mu \approx 600$ cm^2/(Vs). (b) Current I - Voltage V characteristics measured in the same device at different V_g (from V_g = 0 V (purple) to V_g = -12.5 V (red) with ΔV_g =1.25 steps). The electrical response is characteristic of two back to back Schottky diodes generated at the interface between the metallic electrodes and the **Viol**@oSWNT. [Inset] Schematic circuit representing a gold|**Viol**@oSWNT|gold FET mediated by Schottky barriers.

Figure 4a shows the transfer characteristics of three multi-electrode devices made of **Viol**@oSWNT (golden), **Viol**-SWNT (blue) and oSWNT (black). The source-drain current I is measured as a function of a gate voltage V_g applied to the Si substrate while the source-drain bias voltage is fixed to V_{sd} = 0.5 V. The current saturates to almost 10^{-5} A at negative V_g. Above a threshold voltage V_{th} = -3 V, the current abruptly drops around six orders of magnitude and remains below the noise level of the electronics (< 10^{-11} A). The inset in Figure 4a shows I in a linear-scale from where V_{th} is obtained. The hole-carrier depletion at positive gate voltages is a clear indicative of a p-doped semiconductor-like behavior of the **Viol**@oSWNT. Additional samples are shown in the Supporting Information. This is in sharp contrast with the metallic transfer characteristic of bare oSWNT, i.e. without **Viol** molecules, where only a slight gate dependence is observed. The encapsulation of **Viol** molecules therefore tunes the electronic structure of the tubes from metallic to semiconductor. In other words, a gap in the band structure of the tubes is open. A similar effect has been observed in metallic SWNT doped by boron/nitrogen substitution of carbon atoms[21] and has been proposed for tubes modified with molecules in supramolecular configuration.[22] However, the first geometry dramatically changes the composition of the tubes whereas the second is not stable under external manipulation of the devices. In contrast, note that several **Viol**@oSWNT (of the order of 10) are probed simultaneously in the same multielectrode FET. For the device to be depletable with gate, all the connected nanotubes must be semiconducting. The presence of one or several metallic tubes linking a pair of electrodes would result in a residual current at positive V_g that would mask the semiconducting behavior. This is actually the case in a few devices where the spurious metallic nanotubes could be controllably burned out. The encapsulated geometry is therefore rather homogeneous (as seen in the TEM images in Figure 3a), robust to external manipulation like washing, and keeps the SWNT surface clean for the attachment of functional molecules for the fabrication of more complex devices.

The analysis of the transfer characteristic in Figure 4a shows an on-off current ratio of around $I_{on}/I_{off} = 10^6$ and a FET mobility $\mu \approx 600$ cm^2/Vs (See Supporting Information for details). These values are comparable or better than most reported for semiconducting SWNTs functionalized with molecules,[23] indicating that the opening of a band gap by the 'soft' encapsulation of molecules preserves the transport properties of the tubes. The p-doped character of the device could be explained by the strong electron affinity of the V^{2+} molecules but it could also be associated to the typically lower work functions in graphite-like materials compared to gold.[24] As a sanity check, the same experimental process, including a thorough cleaning of the device, has been reproduced for the supramolecular **Viol**-SWNT. Only metallic behavior has been observed in the devices even after controlled burning of some metallic tubes (see Figure 4a). The electronic structure of the SWNT is apparently less sensitive to supra **Viol** or, alternatively, the molecules are washed away in the preparation of the devices.

Figure 4b shows the I-V characteristics measured in the same **Viol**@oSWNT device at different V_g around V_{th}. Under forward bias conditions (V_{sd} > 0) the current rapidly increases and saturates at increasingly higher I for increasing V_g. Under low reverse bias conditions (-1 < V_{sd} < 0) the current remains blocked at $|I_l| \approx 27$ nA. Thereafter $|I|$ abruptly increases and is modulated by V_g. This electrical response is characteristic of a two back-to-back diodes circuit as sketched in Figure 4b. The low forward voltage drop (~0.1 V) and the relative high current leakage I_l point to two Schottky diodes generated at the interface barrier between the metallic Au electrodes and the semiconducting **Viol**@oSWNT. The low forward voltage drop is, in addition, characteristic of p-doped based Schottky diodes, in agreement with the transfer characteristic in Figure 4(c). This diode-like behavior is a further proof of the rather homogeneous

semiconducting behavior of the **Viol**@oSWNT when compared with the linear and symmetric *I-V* curves obtained in oSWNT and **Viol**-SWNT junctions, as expected for metal-metal contacts (see Figure S4 in the Supporting Information).

Several mechanisms may contribute to the band gap opening. One could be the local field induced by the cation, or alternatively the partial hybridization of the molecular orbitals with the band structure of the tube.[25] Additionally, mechanical deformations induced by molecules in SWNTs could modify their electronic bands. To understand the role of the charges, we synthesized a neutral structural analogue of **Viol** featuring alkylated biphenyl moieties, **Biphenyl**@oSWNT system. The preliminary electronic characterization (see Supporting Information) indicates that although certain semiconducting-like behavior is observed, the on/off ratios are drastically reduced pointing to an important role of the cation charge. A more thorough study will be the subject of a future follow-up manuscript.

In conclusion, **Viol** molecules were successfully encapsulated in SWNTs. The filling of the carbon nanotubes was confirmed by TGA, Raman spectroscopy, and crucially by AC-HRTEM. The encapsulation tunes the electronic properties of the nanotube-based FET devices, from metallic to high-quality semiconductor. Such tuning is not observed in analogous supramolecular derivatives. The resulting back-to-back diode circuits could be exploited as tunable rectifiers or current limiters to protect more complex SWNT or molecule-based electronic circuits.

Acknowledgements

We thank Dr. Andrés Castellanos-Gómez (Instituto de Ciencia de Materiales de Madrid) for fruitful discussions. We thank Dr. Daniel Granados and Dr. Manuel Rodriguez for the help with the nanofabrication. We thank Dr. Prabhash Mishra for initial studies on dielectrophoresis. The research leading to these results has received funding from the European Research Council under the European Union's Seventh Framework Programme (FP/2007-2013)/ERC Grant Agreements No. 307609 (ERC Starting Grant "MINT"). We thank the Ministerio de Economía, Industria y Competitividad (Spain) (CTQ2014-60541-P and JdC-2015-23531). E.B. thanks the AMAROUT-II fellowship (Marie Curie Action, FP7-PEOPLE-2011-COFUND). We thank National Centre for Electron Microscopy (ICTS-CNME, Universidad Complutense) for aberration corrected electron microscopy facilities

Keywords: nanotubes • viologen • encapsulation • electronic band gap • FET

[1] a)R. H. Baughman, A. A. Zakhidov, W. A. de Heer, *Science* **2002**, *297*, 787-792; b)Z. Liu, L. Jiao, Y. Yao, X. Xian, J. Zhang, *Adv. Mater.* **2010**, *22*, 2285-2310.

[2] a)Y. He, H. Jin, S. Qiu, Q. Li, *Chem. Comm.* **2017**, *53*, 2934-2937; b)C. Chen, C. Song, J. Yang, D. Chen, W. Zhu, C. Liao, X. Dong, X. Liu, L. Wei, N. Hu, R. He, Y. Zhang, *Nano Energy* **2017**, *32*, 280-286; c)J. Wan, Y. Xu, B. Ozdemir, L. Xu, A. B. Sushkov, Z. Yang, B. Yang, D. Drew, V. Barone, L. Hu, *ACS Nano* **2017**, *11*, 788-796.

[3] a)E. K. Wujcik, C. N. Monty, *Wiley Interdiscip. Rev. Nanomed. Nanobiotechnol.* **2013**, *5*, 233-249; b)G. Bardi, in *Nanomedicine and the Nervous System*, Science Publishers, **2012**, pp. 3-16.

[4] a)H. Kataura, Y. Kumazawa, Y. Maniwa, I. Umezu, S. Suzuki, Y. Ohtsuka, Y. Achiba, *Synth. Met.* **1999**, *103*, 2555-2558; b)M. S. Dresselhaus, G. Dresselhaus, R. Saito, A. Jorio, *Phys. Rep* **2005**, *409*, 47-99.

[5] a)R. Saito, A. R. T. Nugraha, E. H. Hasdeo, N. T. Hung, W. Izumida, *Top. Curr. Chem.* **2017**, *375*, 7; b)T. W. Odom, J.-L. Huang, P. Kim, C. M. Lieber, *Nature* **1998**, *391*, 62-64; c)C. N. R. Rao, B. C. Satishkumar, A. Govindaraj, M. Nath, *ChemPhysChem* **2001**, *2*, 78-105; d)E. Bekyarova, M. E. Itkis, N. Cabrera, B. Zhao, A. Yu, J. Gao, R. C. Haddon, *J. Am. Chem. Soc.* **2005**, *127*, 5990-5995.

[6] a)G. Guanghua, Ç. Tahir, A. G. William, III, *Nanotechnology* **1998**, *9*, 184; b)N. Khandoker, S. C. Hawkins, R. Ibrahim, C. P. Huynh, F. Deng, *Procedia Eng.* **2011**, *10*, 2572-2578.

[7] a)P. Singh, S. Campidelli, S. Giordani, D. Bonifazi, A. Bianco, M. Prato, *Chem. Soc. Rev.* **2009**, *38*, 2214-2230; b)A. Hirsch, *Angew. Chem. Int. Ed.* **2002**, *41*, 1853-1859.

[8] J. L. Bahr, J. M. Tour, *J. Mater. Chem.* **2002**, *12*, 1952-1958.

[9] a)Y.-L. Zhao, J. F. Stoddart, *Acc. Chem. Res.* **2009**, *42*, 1161-1171; b)G. Gavrel, B. Jousselme, A. Filoramo, S. Campidelli, in *Making and Exploiting Fullerenes, Graphene, and Carbon Nanotubes* (Eds.: M. Marcaccio, F. Paolucci), Springer Berlin Heidelberg, Berlin, Heidelberg, **2014**, pp. 95-126.

[10] a)S. Leret, Y. Pouillon, S. Casado, C. Navio, A. Rubio, E. M. Perez, *Chem. Sci.* **2017**, 1927-1935; b)A. de Juan, M. Mar Bernal, E. M. Pérez, *ChemPlusChem* **2015**, *80*, 1153-1157; c)A. de Juan, Y. Pouillon, L. Ruiz-González, A. Torres-Pardo, S. Casado, N. Martín, Á. Rubio, E. M. Pérez, *Angew. Chem. Int. Ed.* **2014**, *53*, 5394-5400; d)A. Lopez-Moreno, E. M. Perez, *Chem. Comm.* **2015**, *51*, 5421-5424.

[11] a)D. A. Britz, A. N. Khlobystov, *Chem. Soc. Rev.* **2006**, *35*, 637-659; b)J. Campo, Y. Piao, S. Lam, C. M. Stafford, J. K. Streit, J. R. Simpson, A. R. Hight Walker, J. A. Fagan, *Nanoscale* **2016**, *1*, 317-324; c)R. Kitaura, N. Imazu, K. Kobayashi, H. Shinohara, *Nano Letters* **2008**, *8*, 693-699; d)M. Hart, E. R. White, J. Chen, C. M. McGilvery, C. J. Pickard, A. Michaelides, A. Sella, M. Shaffer, C. G. Salzmann, *Angew. Chem. Int. Ed.*, n/a-n/a.

[12] A. de Juan, E. M. Perez, *Nanoscale* **2013**, *5*, 7141-7148.

[13] a)C. L. Bird, A. T. Kuhn, *Chem. Soc. Rev.* **1981**, *10*, 49-82; b)M. Suzuki, N. D. Morris, T. E. Mallouk, *Chem. Comm.* **2002**, 1534-1535; c)P. M. S. Monk, *The viologens: physicochemical properties, synthesis, and applications of the salts of 4,4'-bipyridine*, Wiley, England, **1998**.

[14] S. M. Kim, J. H. Jang, K. K. Kim, H. K. Park, J. J. Bae, W. J. Yu, I. H. Lee, G. Kim, D. D. Loc, U. J. Kim, E.-H. Lee, H.-J. Shin, J.-Y. Choi, Y. H. Lee, *J. Am. Chem. Soc.* **2009**, *131*, 327-331.

[15] a)S. Cambré, J. Campo, C. Beirnaert, C. Verlackt, P. Cool, W. Wenseleers, *Nat Nano* **2015**, *10*, 248-252; b)P. Horn, M. Kertesz, *J. Phys. Chem. C.* **2010**, *114*, 12139-12144; c)K. Yanagi, K. Iakoubovskii, H. Matsui, H. Matsuzaki, H. Okamoto, Y. Miyata, Y. Maniwa, S. Kazaoui, N. Minami, H. Kataura, *J. Am. Chem. Soc.* **2007**, *129*, 4992-4997; d)K. Yanagi, Y. Miyata, H. Kataura, *Adv. Mater.* **2006**, *18*, 437-441.

[16] a)T. Zoberbier, T. W. Chamberlain, J. Biskupek, N. Kuganathan, S. Eyhusen, E. Bichoutskaia, U. Kaiser, A. N. Khlobystov, *J. Am. Chem. Soc.* **2012**, *134*, 3073-3079; b)T. W. Chamberlain, J. C. Meyer, J. Biskupek, J. Leschner, A. Santana, N. A. Besley, E. Bichoutskaia, U. Kaiser, A. N. Khlobystov, *Nat. Chem.* **2011**, *3*, 732-737; c)J. H. Warner, Y. Ito, M. H. Rümmeli, B. Büchner, H. Shinohara, G. A. D. Briggs, *ACS Nano* **2009**, *3*, 3037-3044.

[17] R. F. Egerton, P. Li, M. Malac, *Micron* **2004**, *35*, 399-409.

[18] T. W. Chamberlain, J. Biskupek, S. T. Skowron, P. A. Bayliss, E. Bichoutskaia, U. Kaiser, A. N. Khlobystov, *Small* **2015**, *11*, 622-629.

[19] a)X. Q. Chen, T. Saito, H. Yamada, K. Matsushige, *Appl. Phys. Lett.* **2001**, *78*, 3714-3716; b)L. A. Nagahara, I. Amlani, J. Lewenstein, R. K. Tsui, *Appl. Phys. Lett.* **2002**, *80*, 3826-3828; c)K. Yamamoto, S. Akita, Y. Nakayama, *J. Phys. D: Appl. Phys.* **1998**, *31*, L34-L36.

[20] T. Brintlinger, Y.-F. Chen, T. Dürkop, E. Cobas, M. S. Fuhrer, J. D. Barry, J. Melngailis, *Appl. Phys. Lett.* **2002**, *81*, 2454-2456.

[21] Z. Xu, W. Lu, W. Wang, C. Gu, K. Liu, X. Bai, E. Wang, H. Dai, *Adv. Mater.* **2008**, *20*, 3615-3619.

[22] A. K. Manna, S. K. Pati, *Nanoscale* **2010**, *2*, 1190-1195.
[23] a)V. Derenskyi, W. Gomulya, W. Talsma, J. M. Salazar-Rios, M. Fritsch, P. Nirmalraj, H. Riel, S. Allard, U. Scherf, M. A. Loi, *Adv. Mater.* **2017**, 1606757; b)C. Biswas, S. Y. Lee, T. H. Ly, A. Ghosh, Q. N. Dang, Y. H. Lee, *ACS Nano* **2011**, *5*, 9817-9823.
[24] S. J. Tans, A. R. M. Verschueren, C. Dekker, *Nature* **1998**, *393*, 49-52.
[25] O. O. Ogunro, C. I. Nicolas, E. A. Mintz, X.-Q. Wang, *ACS Macro Lett.* **2012**, *1*, 524-528.

Entry for the Table of Contents

Layout 2:

COMMUNICATION

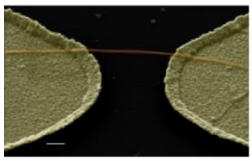

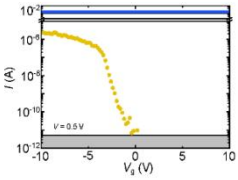

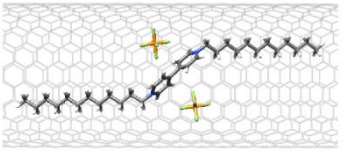

B. Nieto-Ortega J. Villalva, M. Vera-Hidalgo, L. Ruiz-González, E. Burzurí and E. M. Pérez**

Page No. – Page No.

Band gap opening in metallic single-walled carbon nanotubes by encapsulation of an organic salt

Bandgap, be opened! The encapsulation of viologen salts within the tube tunes the electronic band gap of the tube from metallic to a high-quality semiconductor.